

# Decoherence and dissipation during a quantum XOR gate operation

Michael Thorwart<sup>1,2</sup> and Peter Hänggi<sup>1</sup>

<sup>1</sup> *Institut für Physik - Universität Augsburg, Universitätsstr. 1, 86135 Augsburg, Germany*

<sup>2</sup> *Department of Applied Physics, Delft University of Technology, Lorentzweg 1, 2628 CJ Delft, The Netherlands*

(Date: October 27, 2018)

The dynamics of a quantum XOR gate operation in a two-qubit system being coupled to a bath of quantum harmonic oscillators is investigated. Upon applying the numerical quasiadiabatic propagator path integral method, we obtain the numerically precise time-resolved evolution of this interacting two-qubit system in presence of time-dependent external fields without further approximations. We simulate the dissipative gate operation for characteristic experimental realizations of condensed matter qubits; namely, the flux and charge qubits realized in superconducting Josephson systems and qubits formed with semiconductor quantum dots. Moreover, we study systematically the quality of the XOR gate by determining the four characteristic gate quantifiers: fidelity, purity, the quantum degree, and the entanglement capability of the gate. Two different types of errors in the qubits have been modelled, i.e., bit-flip errors and phase errors. The dependence of the quality of the gate operation on the environmental *temperature*, on the *friction strength* stemming from the system-bath interaction, and on the strength of the *interqubit coupling* is systematically explored: Our main finding is that the four gate quantifiers depend only weakly on temperature, but are rather sensitive to the friction strength.

PACS: 03.67.Lx, 03.65.Yz, 89.70.+c, 05.30.-d, 05.40.-a

## I. INTRODUCTION

The basic elements of quantum computation are logic quantum gates which represent manipulations of quantum bits,  $|0\rangle$  and  $|1\rangle$ , according to Boolean algebra. Any arbitrary complex logic operation can be build up of only a few basic gates (*universal gates*) [1] and one can show that almost every gate which operates on two or more qubits is a universal gate [2]. The explicit construction of quantum networks for elementary arithmetic operations then becomes possible upon appropriately combining such universal gates; see, for instance, Ref. [3] for the explicit construction of the addition or the modular exponentiation. In turn, this permits the implementation of Shor's quantum factorizing algorithm [4] in terms of elementary gates. Together with Deutsch's algorithm [5], these two quantum algorithms are presently the most important examples which are known to be superior to their classical counterparts and which do justify the current efforts towards a technological realization of a quantum computer.

In this work we concentrate on one such elementary gate, namely the *quantum exclusive OR (XOR) gate*. It is a unitary transformation which propagates an initial state  $|\Psi_{\text{in}}\rangle$  of a two-qubit system to a final state  $|\Psi_{\text{out}}\rangle = U_{\text{XOR}}|\Psi_{\text{in}}\rangle$ . Represented in the computational basis  $|b_i\rangle \in \{|00\rangle, |01\rangle, |10\rangle, |11\rangle\}$  ( $i = 1, \dots, 4$ ), the XOR gate operation can be written as

$$U_{\text{XOR}} = \begin{pmatrix} 1 & 0 & 0 & 0 \\ 0 & 1 & 0 & 0 \\ 0 & 0 & 0 & 1 \\ 0 & 0 & 1 & 0 \end{pmatrix}. \quad (1)$$

Since this operation inverts the state of the second qubit of the basis states if the first qubit is in the state  $|1\rangle$ , this operation is also called the *quantum controlled NOT (CNOT) gate*. The set of all one-qubit gates together with the quantum XOR gate is universal, as has been demonstrated in Ref. [6].

The main impediment on the roadway to a working quantum computer is decoherence [7–12]. It disturbs the phase relation in a quantum superposition state and therefore is effective at the roots where the quantum computer is believed to have its most important advantage. Any realistic quantum computer will have some interaction with its environment which induces decoherence (decay of the off-diagonal elements of the reduced density matrix) and dissipation (change of populations of the reduced density matrix). Moreover, other sources for decoherence which are due to imperfect gate operations and to cross-talks of the qubits within a register need to be considered [10].

Several previous works in the literature deal with the effect of decoherence in quantum information processing systems. Unruh [7] and Palma *et al.* [9] consider a model of a single qubit which is represented by the eigenstates of the quasi-spin operator  $\sigma_z$  and which couples to a bosonic environment via its  $\sigma_z$ -component. It describes appropriately

the dephasing (decoherence) but does not include population exchange (dissipation). Combining  $L$  *non-interacting* qubits of this type, they estimate the decoherence (in the limit of a large coherence length of the bath) to increase exponentially with the length  $L$  of the register.

Dissipative effects (bit flip errors) are properly described by the so-called spin-boson model [13–16], where the qubit is represented by the  $\sigma_x$ -component of the spin-1/2, but the coupling to the bosonic bath is mediated by the  $\sigma_z$ -component of the spin-1/2 (note, that this refers to the localized representation). In this model, the bath also induces transitions between the two system eigenstates (bit flips) and – in addition to decoherence – energy is exchanged between system and bath. The general solution of the problem in terms of a generalized (non-Markovian) master equation for the entire reduced density matrix for an arbitrary initial preparation in presence of a static bias and also for a time-dependent driving has been given in Ref. [16]. In our work, the assumption of a Markovian bath and of a weak system-bath interaction (Bloch-Redfield approach), which may restrict the validity of the master equation (see below), is not made.

The previously discussed works concern the investigation of decoherence in single qubits or in a register of non-interacting qubits. Decoherence and dissipation in a system of *interacting* qubits has been studied only rarely. The dynamics of two coupled two-level systems has been investigated by Dubé and Stamp [17] by means of a general model for coupled Josephson junctions, for coupled nanomagnets or for interacting Kondo impurities. Each two-level system is represented (in the tunneling representation) by the  $\sigma_x$ -component of a spin-1/2. The two spins interact via their  $\sigma_z$ -components. Moreover, their  $\sigma_z$ -components couple to a bosonic bath. By use of real-time path integrals the dynamics of the relaxation process is determined. Although no specific problem of quantum information processing is investigated, this is the first work where two interacting spins in a dissipative bath have been considered.

A similar model has been studied by Governale, Grifoni and Schön [18]. Two biased spin-1/2 systems interact via their  $\sigma_y$ -components which is the appropriate coupling for Josephson junction charge qubits (see below). Moreover, their  $\sigma_z$ -components couple either to the same or to different bosonic baths. Applying the widely used Bloch-Redfield formalism, the time evolution of the populations of the logical states is evaluated. This model describes dissipation being caused by fluctuations in voltage sources in Josephson junction charge qubits (see below). However, no specific quantum information operation has been considered.

A two-qubit quantum gate for quantum information processing in coupled quantum dots has been investigated in Refs. [11,19]. Two spin-1/2 systems are coupled using a time-dependent Heisenberg-type interaction. Moreover, a coupling of the spins to a bosonic bath has been taken into account. By solving the quantum Liouville equation in the limit of weak system-bath coupling (Born-Markov approximation) for the reduced density operator, the purity and the fidelity of the swap operation  $U_{\text{swap}}|ij\rangle = |ji\rangle$  ( $i, j = 0, 1$ ) is calculated as a function of time. However, the authors consider the time-evolution of the quantum system *after the swap operation has been completed*. The same is true for the XOR gate operation in Ref. [11], where, additionally, a further assumption has been made: The pulse sequence to realize the quantum XOR consists of four pulses of the external fields. Each pulse is taken to be constant over the corresponding time interval. To obtain the solution over the entire time span within the Born-Markov approximation, it is necessary to assume a finite time interval between the single pulses. This is required because the Born-Markov approximation is known to violate positivity of the reduced density operator at short transient times [20,21]. This additional time span (pulse-to-pulse time) has been taken as three times the switching time interval. This leads to an extension of the computation time which is only due to formal mathematical reasons and which deteriorates the quality of the gate operation. Moreover, a systematic study of the dependence of the gate quantifiers on the relevant parameters has not been given.

In this work, we investigate systematically the XOR quantum gate in presence of an interaction of the qubits with their environment. Thereby, we take into account the full time-dependence of the external fields which induce the XOR operation without invoking further approximations on the system Hamiltonian. In particular, we use the numerical *ab-initio* technique of the quasiadiabatic propagator path integral (QUAPI) [22] (for other applications, see also Refs. [23,24]). This numerically precise iterative real-time path integral method does not suffer from the above mentioned problem of lacking positivity. In order to realize the logic XOR operation in physical systems, we introduce a generic model Hamiltonian which is suitable for studying the XOR operation on a very general and idealized level. We determine the quality of the gate by calculating the four characteristic gate quantifiers introduced by Poyatos, Cirac and Zoller [25]: namely, the (i) purity, (ii) fidelity, (iii) quantum degree, and (iv) entanglement capability. To that end, we consider two important types of computational errors, i.e., phase errors and bit flip errors. The former can be modelled by coupling the  $\sigma_z$ -component of each spin to the bath while the later is induced by coupling the  $\sigma_x$ -component of each spin to the bath. We are mainly interested in the quality of the gate operation during its time evolution and, most importantly, right after it has been completed. Our analysis covers a wide field of physical systems and we choose parameter sets which mimic the realistic physical situation for flux qubits or charge qubits proposed in superconducting hybrid systems as well as charge and spin states in coupled semiconductor quantum dots (see below).

So far, we have discussed theoretical aspects of quantum information processing. However, those refined and highly

elaborate concepts face the question of how they can be implemented in experimental hardware. Several proposals to build a quantum information processor exist. Prominent candidates are, for instance, atoms in optical cavities, ions in linear or Paul traps interacting with laser beams, or nuclear spins in an NMR liquid [26]. Although the experimental techniques in those fields of research are currently most advanced, the problem of upscaling of a quantum computer can seemingly only be solved within condensed matter systems which can be embedded in an electronic circuit. Prominent systems for condensed matter qubits are flux states of a superconducting quantum interference device (*flux qubits*) [27] (see also [12]), charge states of superconducting islands with Josephson junctions (*charge qubits*) [12,28], and spin [11,29] or charge [30] states in ultrasmall coupled semiconductor quantum dots (*quantum dot qubits*). Moreover, several realizations of qubits in nuclear [31,32] and electronic [32,33] spins in semiconductor nanostructures have been proposed. In this work, we concentrate on typical experimental situations for flux and charge qubits in Josephson junction devices and for charge qubits in coupled quantum dots.

The paper is organized as follows: In the subsequent Section II, we introduce a generic model as a starting point for the quantum XOR operation including the interaction with the environment. In Section III, we present a brief review on the numerical technique of the quasiadiabatic propagator path integral (QUAPI) which we employ in the following. In order to determine the quality of the decoherent XOR gate, we use four quantifiers which are introduced in Section IV. The results and the conclusions are presented in Sec. V and Sec. VI, respectively.

## II. A GENERIC MODEL FOR THE QUANTUM XOR GATE

### A. The coherent XOR operation

The quantum XOR gate is a two-qubit operation which can be modelled by two coupled spin-1/2 systems represented by the Pauli operators  $\vec{\sigma}_j = (\sigma_j^x, \sigma_j^y, \sigma_j^z)^T, j = 1, 2$ . The two logical states of each qubit are represented by the two eigenstates of the  $\sigma_z$ -component of each spin, i.e.,  $|0\rangle_j \equiv |\uparrow\rangle_j$  and  $|1\rangle_j \equiv |\downarrow\rangle_j$ . We assume that the single qubit as well as the coupling between the two qubits can be controlled by switching on (local) external fields, for instance, magnetic fields. This system can generically be described [12] by the Hamiltonian

$$H_{\text{XOR}}(t) = -\frac{\hbar}{2} \sum_{j=1}^2 \vec{B}_j(t) \vec{\sigma}_j + \hbar \sum_{j \neq k} J(t) \sigma_j^+ \sigma_k^- . \quad (2)$$

where  $\sigma_j^\pm = (\sigma_j^x \pm i\sigma_j^y)/2$ . Moreover,  $\vec{B}_j(t) = (B_j^x(t), 0, B_j^z(t))^T, j = 1, 2$  are time-dependent coupling strengths (with the dimension of a frequency) arising from local time-dependent external fields at the site of the spin  $j$  in longitudinal ( $z$ -) or transverse ( $x$ -) direction. In Eq. (2), the coupling between the two qubits is assumed to be symmetric; furthermore it should be controllable from the outside leading to a time-dependent interaction strength  $J(t)$ . The particular form of the interaction in Eq. (2) is only one example. We note that this generic model does not account for the particular details of a physical realization of qubits in a specific condensed matter system. For each individual system, such as flux qubits or charge qubits, the Hamiltonian looks different in detail. In particular, the coupling term between the two qubits takes different forms. However, the differences to our generic model in Eq. (2) are of minor influence only. The general physical behavior will be similar such that our generic model serves as an archetype.

The quantum XOR gate (1) can be obtained by a sequence of one- and two-qubit operations according to [12]

$$U_{\text{XOR}} = U_2^x \left( \frac{\pi}{2} \right) U_2^z \left( -\frac{\pi}{2} \right) U_2^x (-\pi) U_{12} \left( -\frac{\pi}{2} \right) U_1^x \left( -\frac{\pi}{2} \right) \\ \times U_{12} \left( \frac{\pi}{2} \right) U_1^z \left( -\frac{\pi}{2} \right) U_2^z \left( -\frac{\pi}{2} \right) , \quad (3)$$

where

$$U_j^{x/z}(\alpha) = \exp \left( i \frac{\alpha}{2} \sigma_j^{x/z} \right) , \quad j = 1, 2, \\ U_{12}(\beta) = \exp \left( i\beta(\sigma_1^+ \sigma_2^- + \sigma_1^- \sigma_2^+) \right) \quad (4)$$

are the propagators over the single time-intervals with the external fields in the Hamiltonian, Eq. (2), switched on and off in the following way: In order to attain this propagator, a pulse sequence of the external fields is necessary. For simplicity we assume throughout this work, that the pulses are switched instantaneously on and off and are constant over the time span  $t_{\text{off}} - t_{\text{on}}$  they are on. This induces time-dependent interaction strengths  $\mathcal{B}(t) = \mathcal{B}[\Theta(t - t_{\text{on}}) -$

$\Theta(t - t_{\text{off}})]$  with  $\mathcal{B} = B_j^{(x/z)}$ ,  $J = \text{const.}$  and with  $\Theta(t)$  being the Heaviside function. Furthermore, we assume that both spins are equal and experience local fields of equal strength. This implies  $B_1^{x/z} = B_2^{x/z} \equiv B^{x/z}$ . The angles  $\alpha$  and  $\beta$  in Eq. (4) are related to the actual physical propagation time  $t$  according to

$$\alpha = B^{x/z}t \quad \text{und} \quad \beta = Jt. \quad (5)$$

The switching times then follow as  $t_1 = \pi/(2B^z)$ ,  $t_2 = t_1 + \pi/(2J)$ ,  $t_3 = t_2 + \pi/(2B^x)$ ,  $t_4 = t_3 + \pi/(2J)$ ,  $t_5 = t_4 + \pi/(B^x)$ ,  $t_6 = t_5 + \pi/(2B^z)$  and  $t_{\text{XOR}} = t_6 + \pi/(2B^x)$ , where  $t_{\text{XOR}}$  denotes the total time elapsed during the full XOR gate operation. An example of this pulse sequence is sketched in Fig. 1 for the case of  $B^x = B^z = J$ . The coupling constants are given in units of  $B^z$  while the time is scaled in units of  $(B^z)^{-1}$ . One immediately observes that the computation time  $t_{\text{XOR}}$  is extended if the coupling energies are decreased. We note that the assumption of rectangular pulses is not required by the numerical technique we use and is made here only for the sake of simplicity. We could also consider other shapes of the pulses which are more realistic for specific physical systems, and especially, we could consider imperfect switching processes as well; the latter would constitute a further source of decoherence.

## B. Interaction with the environment

We model the interaction of the qubit system with the fluctuating environment by a Hamiltonian, in which  $H_{\text{XOR}}(t)$  is coupled to a bath of harmonic oscillators, i.e.,

$$H(t) = H_{\text{XOR}}(t) + H_{\text{B}} + H_{\text{int}}^{x/z}, \quad (6)$$

with

$$H_{\text{B}} = \sum_{j=1}^N \hbar \omega_j \left( a_j^\dagger a_j + \frac{1}{2} \right). \quad (7)$$

Here,  $a_j^\dagger (a_j)$  denotes the creation (annihilation) operator of the  $j$ -th bath oscillator with frequency  $\omega_j$ . Since we want to investigate the role of bit-flip errors as well as phase errors we include in our model two different types of interactions: On the one hand, the  $\sigma^x$ -components of the spins couple to the fluctuating environment and the populations of the qubit states are disturbed (bit-flip errors). On the other hand, phase errors are generated by a coupling of the  $\sigma^z$ -components of the spins to the environmental noise. This is conveniently modelled by the form

$$H_{\text{int}}^{x/z} = \frac{\hbar}{2} \left( \sigma_1^{x/z} + \sigma_2^{x/z} \right) \sum_{j=1}^N \kappa_j^{x/z} (a_j^\dagger + a_j), \quad (8)$$

where  $\kappa_j^{x/z}$  denotes the coupling strength of the  $j$ -th oscillator to the system and where the superscript  $(x/z)$  denotes *either the one or the other kind of interaction*. We note that we assume here, to keep things simple, a coupling of the two spins to the same bath. This implies that the spins are effectively coupled to each other via the bath. A coupling of the spins to different (uncorrelated) baths could be readily incorporated in the numerical QUAPI technique (see below).

To study the dynamics of this system, we have to specify the initial conditions. Throughout this work, we assume that the density operator  $W(t)$  of the entire system-plus-bath at initial time  $t = 0$  factorizes according to

$$W(0) = \rho_{\text{S}}(0) \otimes \rho_{\text{B}}. \quad (9)$$

$\rho_{\text{S}}(0)$  is the density operator of the system at time  $t = 0$  and  $\rho_{\text{B}} = Z_{\text{B}}^{-1} \exp(-H_{\text{B}}/(k_{\text{B}}T))$  is the canonical equilibrium distribution of the (decoupled) bath at temperature  $T$ . Moreover,  $Z_{\text{B}} = \text{tr} \exp(-H_{\text{B}}/(k_{\text{B}}T))$  and  $k_{\text{B}}$  denotes the Boltzmann constant.

The influence of the bath is fully characterized [14] by the spectral density

$$\Gamma^{x/z}(\omega) = 2\pi \sum_{j=1}^N (\kappa_j^{x/z})^2 \delta(\omega - \omega_j) \quad (10)$$

which assumes a continuous form if the number  $N$  of oscillators approaches infinity. Throughout this work, we apply an Ohmic spectral density with an exponential cut-off, i.e.,

$$\Gamma^{x/z}(\omega) = \gamma^{x/z} \omega \exp(-\omega/\omega_c), \quad (11)$$

where the dimensionless damping parameter  $\gamma^{x/z}$  characterizes the strength of the interaction with the environment. This spectrum mimics the environmentally induced fluctuations in the external circuit which supplies flux through the SQUID loops in the flux qubits [12,27]. Moreover, background charge fluctuations in the voltage sources in Josephson charge qubits [12,28] also lead to an Ohmic impedance  $R$ . Similarly, electronic states in coupled quantum dot qubits experience an Ohmic environment, either for the spin [11,29] or for the charge [30] degrees of freedom.

### III. NUMERICAL AB-INITIO TECHNIQUE: QUAPI

In order to describe the dynamics of the two-qubit system of interest it is sufficient to consider the time evolution of the reduced density operator

$$\begin{aligned} \rho(t) &= \text{tr}_{\text{bath}} \mathcal{U}(t, 0) W(0) \mathcal{U}^{-1}(t, 0) , \\ \mathcal{U}(t, 0) &= \mathcal{T} \exp \left\{ -i/\hbar \int_0^t H(t') dt' \right\} . \end{aligned} \quad (12)$$

Here,  $\mathcal{U}(t, 0)$  is the propagator of the full system-plus-bath and  $\mathcal{T}$  denotes the time-ordering operator. Moreover,  $\text{tr}_{\text{bath}}$  means the partial trace over the harmonic bath oscillators. Due to our assumption that the bath is initially at thermal equilibrium and decoupled from the system, see Eq. (9), the partial trace over the bath can be performed. We denote the matrix elements of the reduced density matrix in the computational basis with  $\rho_{ij}(t) \equiv \langle b_i | \rho(t) | b_j \rangle$  and rewrite them according to Feynman and Vernon [34] as

$$\rho_{ij}(t) = \sum_{m,n=1}^4 G_{ij,mn}(t, 0) \rho_{mn}(0) , \quad (13)$$

with the propagator  $G$  given by

$$G_{ij,mn}(t, 0) = \int \mathcal{D}x \mathcal{D}x' \mathcal{A}[x] \mathcal{A}^*[x'] \mathcal{F}_{FV}[x, x'] . \quad (14)$$

The functional  $\mathcal{A}[x]$  denotes the probability amplitude for the free system to follow the path  $x(t)$  and  $\mathcal{F}_{FV}[x, x']$  denotes the Feynman-Vernon influence functional [34] (see Ref. [14] for details). The functional integrations in Eq. (14) extend over paths with endpoints  $x(0) = x_m, x(t) = x_i, x'(0) = x_n$  and  $x'(t) = x_j$  which belong to the initial and final states,  $\rho_{mn}(0)$  and  $\rho_{ij}(t)$ , respectively.

The technique which we use to calculate the reduced density operator Eq. (13) is the iterative tensor multiplication scheme derived for the so-called quasiadiabatic propagator path integral (QUAPI). This numerical algorithm was developed by Makri and Makarov [22] within the context of chemical physics. Since its first applications it has been successfully tested and adopted to various problems of open quantum systems, with and without external driving [22–24]. Because the details of this algorithm has been extensively discussed previously in the literature [22–24], we only mention those prominent ingredients which are of importance for our work:

(i) Symmetric splitting of the short-time propagator: To obtain a numerical iteration scheme, we discretize the time interval  $[0, t]$  into  $\mathcal{N}$  steps  $\Delta t$ , such that  $t_k = k\Delta t$  and split symmetrically the full propagator over one time step  $\mathcal{U}(t_{k+1}, t_k)$  in Eq. (12) according to the Trotter formula into a system and an environmental part:

$$\begin{aligned} \mathcal{U}(t_{k+1}, t_k) &\approx \exp(-iH_B \Delta t / 2\hbar) \mathcal{U}_S(t_{k+1}, t_k) \exp(-iH_B \Delta t / 2\hbar) , \\ \mathcal{U}_S(t_{k+1}, t_k) &= \mathcal{T} \exp \left\{ -\frac{i}{\hbar} \int_{t_k}^{t_{k+1}} dt' H_{\text{XOR}}(t') \right\} . \end{aligned} \quad (15)$$

The neglect of higher order terms of the propagator in Eq. (15) causes an error of the order of  $\Delta t^3$ . The short-time propagator  $\mathcal{U}_S$  of the bare system is given by the corresponding exact system propagators in Eq. (4) over a time step  $\Delta t$ . At this point, we emphasize that this method is not plagued by the problem of lacking positivity of the density operator at short times, as it is the case for the usually employed master equation approach in the Born-Markov limit [11,19]. The *exact* coherent dynamics of the bare system enters and the decomposition of the short-time propagator according to Eq. (15) is valid for any arbitrary short time.

(ii) The interaction with the bath induces correlations among the paths (memory) which are described by the influence functional in Eq. (14). As long as the temperature of the Ohmic bath is finite, these correlations decay exponentially fast with increasing time [14]. This motivates to neglect such long-time correlations and to break up

the influence kernels into smaller pieces of length  $K \Delta t$ , where  $K$  denotes the number of time steps over which the memory is fully taken into account.

The two strategies in (i) and (ii) are countercurrent: In step (i) a small time step  $\Delta t$  is desirable in order to minimize the error due to the neglected higher order terms in the propagator. On the other hand, in (ii) a large time step is wanted in order to take a long memory range into account. A compromise between those two errors has to be found in practice by applying the principle of minimal sensitivity [24] to adjust the two parameters  $\Delta t$  and  $K$ , see discussion below.

(iii) The third important ingredient is the appropriate choice of basis representation of the problem. For the algorithm it is required to iterate the dynamics in the eigenbasis of that system operator which couples to the bath. Then the influence functional in Eq. (14) can be evaluated in terms of the eigenvalues of the coupling operator. In problems where the coordinate of a quantum particle in a continuous potential is damped, the continuous position operator turns into a discrete set of position eigenvalues. Hence, this representation has been termed *discrete variable representation (DVR)*.

*Bit-flip errors:* If the  $\sigma_x$ -components of each spin couple to the bath, see Eq. (8), the eigenbasis of the coupling operator is determined by  $\langle \alpha_i | (\sigma_1^x + \sigma_2^x) / 2 | \alpha_j \rangle = \lambda_i \delta_{ij}$  with  $\lambda_1 = 0, \lambda_2 = -1, \lambda_3 = 1$  and  $\lambda_4 = 0$ . A basis rotation of the computational basis with basis states  $|b_j\rangle$  has to be performed according to

$$|\alpha_i\rangle = \sum_{j=1}^4 R_{ij} |b_j\rangle, \quad (16)$$

with the transformation matrix

$$R = \frac{1}{2} \begin{pmatrix} 1 & 1 & 1 & -1 \\ -1 & -1 & 1 & -1 \\ 1 & -1 & 1 & 1 \\ -1 & 1 & 1 & 1 \end{pmatrix}. \quad (17)$$

*Phase errors:* For the second case that the  $\sigma_z$ -components of each spin couple to the bath in Eq. (8), the system part of Hamiltonian is already diagonal in the computational basis, i.e.,  $\langle b_i | (\sigma_1^z + \sigma_2^z) / 2 | b_j \rangle = \lambda_i \delta_{ij}$  with  $\lambda_1 = 1, \lambda_2 = 0, \lambda_3 = 0$  and  $\lambda_4 = -1$ . No additional basis transformation is necessary.

#### IV. CHARACTERISTIC GATE QUANTIFIERS

In order to quantify the *quality* of the quantum gate, we use four global parameters which have been defined by Poyatos, Cirac and Zoller [25]: (i) the gate fidelity  $\mathcal{F}$ , (ii) the gate purity  $\mathcal{P}$ , (iii) the quantum degree  $\mathcal{Q}$  of the gate, and (iv) the entanglement capability  $\mathcal{C}$  of the gate. These four quantifiers can be calculated once the reduced density operator  $\rho$  in Eq. (12) is determined. To this end, 16 unentangled input states  $|\Psi_{\text{in}}^j\rangle, j = 1, \dots, 16$  are defined according to  $|\psi_a\rangle_1 |\psi_b\rangle_2$  ( $a, b = 1, \dots, 4$ ), with  $|\psi_1\rangle = |0\rangle, |\psi_2\rangle = |1\rangle, |\psi_3\rangle = (|0\rangle + |1\rangle) / \sqrt{2}$  and  $|\psi_4\rangle = (|0\rangle + i|1\rangle) / \sqrt{2}$ . They form one possible basis set and span the Hilbert space for the superoperator  $\mathcal{V}_{\text{XOR}}$  where  $\rho(t_{\text{XOR}}) = \mathcal{V}_{\text{XOR}} \rho(0)$ , see Ref. [25] for details. Moreover, these basis states are chosen to be unentangled states in order to avoid the application of a preceding two-qubit gate for the preparation of the system state.

The gate fidelity  $\mathcal{F}$  is defined as the overlap between the propagation with the ideal propagator  $U_{\text{XOR}}$ , Eq. (1), averaged over all 16 initial states  $|\Psi_{\text{in}}^j\rangle$ , according to

$$\mathcal{F} = \frac{1}{16} \sum_{j=1}^{16} \langle \Psi_{\text{in}}^j | U_{\text{XOR}}^\dagger \rho_{\text{XOR}}^j U_{\text{XOR}} | \Psi_{\text{in}}^j \rangle \quad (18)$$

with  $\rho_{\text{XOR}}^j = \rho(t_{\text{XOR}})$  with initial condition  $\rho(0) = |\Psi_{\text{in}}^j\rangle \langle \Psi_{\text{in}}^j|$ .

In a similar way, the purity  $\mathcal{P}$  is defined as

$$\mathcal{P} = \frac{1}{16} \sum_{j=1}^{16} \text{tr}(\rho_{\text{XOR}}^j)^2. \quad (19)$$

This quantity is proportional to the (negative) linearized entropy and reflects the effects of decoherence.

The third quantity, the quantum degree  $\mathcal{Q}$  of the gate, is defined as the maximum of the overlap of all possible output states stemming from unentangled states and of all maximally entangled (Bell) states  $|\Psi_{\text{me}}^k\rangle, k = 1, \dots, 4$ . In formal terms, this implies

$$\mathcal{Q} = \max_{j,k} \langle \Psi_{\text{me}}^k | \rho_{\text{XOR}}^j | \Psi_{\text{me}}^k \rangle. \quad (20)$$

The purpose of this parameter is to quantify the notion of nonlocality. Bennett and co-workers [35] have shown that all those density operators which have an overlap with a maximally entangled state being larger than the value  $(2 + 3\sqrt{2})/8 \approx 0.78$  are non-local, i.e., violate the Clauser-Horne-Shimony-Holt inequality [35].

Obviously,  $\mathcal{F} = 1, \mathcal{P} = 1, \mathcal{Q} = 1$  denote the ideal gate operation.

The fourth quantifier is the entanglement capability  $\mathcal{C}$  of the gate. It denotes the smallest eigenvalue of the partial transposed density matrix [36] which is determined from  $\rho_{\text{XOR}}^j$  for all unentangled input states  $|\Psi_{\text{in}}^j\rangle$ .  $\rho_{\text{XOR}}^j$  characterizes an entangled state if and only if the smallest eigenvalue of the partial transposed density operator is negative. The ideal operation has an entanglement capability of  $\mathcal{C} = -0.5$ .

## V. RESULTS

Having determined the reduced matrix in Eq. (12) by the iterative QUAPI algorithm, we investigate the influence of the interaction with the environment systematically. Therefore, we assume that the two qubits are identical and experience external fields of the same strength, i.e.,  $B_1^x = B_2^x = B^x$  and  $B_1^z = B_2^z = B^z$ . Moreover, we introduce the following dimensionless parameters: We scale the quantities with respect to the characteristic energy scale of the single qubit which is given by the energy splitting  $\hbar B^z$  of the single qubit. This in turn defines a time scale  $(B^z)^{-1}$ . Consequently, the temperature is given in units of  $\hbar B^z/k_{\text{B}}$  (Note that  $\gamma^{x/z}$  is already dimensionless). For all following results, we have used a cut-off frequency of  $\omega_c = 50B^z$  in (11).

### A. Time resolved quantum XOR operation

We first illustrate the time-resolved dynamics of a generic XOR operation. To this end, we determine the populations of the four states of the computational basis as a function of time, i.e.,  $P_{ij}(t) := \langle ij | \rho(t) | ij \rangle$  with  $i, j = 0, 1$  for the initial condition  $\rho(0) = |11\rangle\langle 11|$ . We choose the pulse sequence sketched in Fig. 1 with parameters set to  $B^x = B^z$  and  $J = B^z$ . Moreover, we choose for illustrative purpose a rather high temperature of  $T = 0.1\hbar B^z/k_{\text{B}}$ . Fig. 2 depicts the results for the three different cases of (i) no damping,  $\gamma^{x/z} = 0$ , (solid line), (ii) bit flip errors with  $\gamma^x = 0.01$  (long dashed line), and (iii) phase errors with  $\gamma^z = 0.01$  (dotted line). The switching times  $t_j$  are equal to multiples of  $\pi/2$  for this special case of equal energies.

The iterative QUAPI algorithm possesses two free parameters which have to be properly adjusted. We fix the number  $K$  of memory time steps and the length  $\Delta t$  of each time step according to the *principle of minimal sensitivity* [24]. By applying this method, we obtain the values  $\Delta t = 0.15(B^z)^{-1}$  with  $K = 2$  (not shown).

As one observes, the final state of the ideal operation ( $\gamma^{x/z} = 0$ ) is  $|\Psi\rangle = |10\rangle$ . The deviation of the dynamics in presence of decoherence and dissipation from the ideal case is clearly visible.

### B. Quality of realistic quantum XOR operations

In order to study realistic physical situations, we apply our method to three different condensed matter systems, namely flux qubits (set I) [27,12], charge qubits (set II) [12,28], and qubits realized in coupled semiconductor quantum dots (set III) [11,29]. We choose typical parameter sets published in the literature. They are summarized in Table I.

The QUAPI parameters are again determined by the principle of minimal sensitivity for  $K = 3$ . We obtain for the case of  $H_{\text{int}}^x$  (bit flip errors) for set I (in units of  $(B^z)^{-1}$ ):  $\Delta t = 0.06$ , for set II:  $\Delta t = 0.2$ , and for set III:  $\Delta t = 0.02$ , and for the case of  $H_{\text{int}}^z$  (phase errors) for set I:  $\Delta t = 0.013$ , for set II:  $\Delta t = 0.08$ , and for set III:  $\Delta t = 0.01$ .

#### 1. Dependence on temperature

The dependence of the four characteristic gate quantifiers on the bath temperature  $T$  is depicted with Fig. 3. In panel a.) the influence of the random bit flips are investigated while the panel b.) depicts the effect of phase errors.

The damping constant for the bit flip errors is chosen to be  $\gamma^x = 10^{-6}$  and for the phase errors we set  $\gamma^z = 10^{-4}$  [12].

First, one observes that all results depend only weakly on temperature. Extrapolating the results to zero temperature indicates the influence of the zero point oscillations of the harmonic bath oscillators. Second, the results for  $\mathcal{F}$ ,  $\mathcal{P}$  and  $\mathcal{Q}$  do in no case exceed a value of 0.999 85 for bit flip errors and 0.975 for phase errors. This demonstrates that even smaller strengths of the coupling to the environment than  $\gamma^x = 10^{-6}$  or  $\gamma^z = 10^{-4}$  are necessary in order to obtain a desired value of 0.999 99 [11]!

Furthermore, we observe that the flux qubits (set I) are the least sensitive to bit flip errors while charge qubits (set II) and quantum dot qubits (set III) both are performing worse, see Fig. 3 a.). On the other hand, quantum dot qubits (set III) are most immune from phase errors, see Fig. 3 b.) while the superconducting systems assume worse results.

## 2. Dependence on the damping strength

As shown in the preceding section, the quality of the gate operation cannot be improved by lowering the temperature of the environment. On the contrary, the shielding of the qubit system against external noise is most important. This is demonstrated by the results for the dependence of the four gate quantifiers on the coupling constants  $\gamma^{x/z}$  depicted in Fig. 4.

We find again that the results for the flux qubits (set I) approach the ideal values of  $\mathcal{F} = \mathcal{P} = \mathcal{Q} = 1$  and  $\mathcal{C} = -0.5$  first upon decreasing the friction strength, see Fig. 4 a.). However, the flux qubits are more sensitive to phase errors from which the quantum dot qubits (set III) are seemingly most immune, see Fig. 4 b.). Note that in Fig. 4 the lower bound of  $\mathcal{Q} \approx 0.78$  for the Clauser-Horne-Shimony-Holt inequality is indicated by the horizontal dotted-dashed line.

For all three systems we find that the damping strength has to be less than  $\gamma^{x/z} \approx 10^{-7}$  in order to serve as suitable candidates for a quantum information processor.

## 3. Dependence on interqubit coupling strength

In the remaining part we address the dependence of the quality of the gate operation on the strength  $J$  of the interqubit coupling. Physically, one expects that a coupling strength which is comparable to the characteristic qubit energy ( $J \approx B^z$ ) would yield the best results. This is confirmed in Fig. 5 for the two different sets I and III (set II is equivalent to set I). The panel a.) illustrates the results for the bit flip errors with  $\gamma^x = 10^{-6}$ , and correspondingly panel b.) for the phase errors with  $\gamma^z = 10^{-4}$ . As one can observe, the superconducting qubits (set I) can perform with a smaller interqubit coupling than the quantum dot qubits (set III). Moreover, the use of an interqubit coupling larger than  $J \approx 10^{-1}B^z$  is advantageous. The horizontal dotted-dashed line in Fig. 5 b.) indicates the lower bound of  $\mathcal{Q} \approx 0.78$  for nonlocality.

## VI. CONCLUSIONS

In this work we have shown that the numerical quasiadiabatic propagator path integral method (QUAPI) of Makri and Makarov provides an appropriate method to investigate decohering quantum information processes which involve time-dependent Hamiltonians in presence of a coupling to an external environment. We have applied this iterative algorithm to the example of the quantum XOR gate operation and have obtained the full time-resolved evolution of the two-qubit system in presence of time-dependent external fields. No further approximations on the time evolution of the gate operation such as a Markovian evolution or extended time spans of the gate operation have been invoked.

We have investigated the quality of the quantum XOR operation by numerically determining four characteristic gate quantifiers, i.e., the fidelity  $\mathcal{F}$ , the purity  $\mathcal{P}$ , the quantum degree  $\mathcal{Q}$ , and the entanglement capability  $\mathcal{C}$  of the gate. We have simulated the gate operation for three parameter sets which mimic realistic experimental situations for condensed matter qubits, such as flux and charge qubits in superconducting Josephson systems and qubits in semiconductor quantum dots. Thereby, we have succeeded to investigate systematically the quality of the gate operation as a function of the environmental temperature  $T$ , the friction strength  $\gamma$ , and the strength  $J$  of the interqubit coupling. Two different types of errors in the qubits have been modelled: (i) bit-flip errors and (ii) phase errors. We have elucidated how the different physical setups perform under these conditions. As major findings we establish that the quality of the gate depends *only weakly on temperature* but rather *strongly on the friction strength*. Moreover, we have



illustrated that the interqubit coupling strength plays an important role and should not be smaller than  $0.1E_0$  with  $E_0$  being the typical energy scale of the qubit system.

In order for a quantum information processor to operate optimally the decoherent influence of the environment needs to be suppressed. Therefore, three different approaches are currently discussed: These are the techniques of quantum error correction, fault tolerant quantum computation, and entanglement purification [26]. The general idea common to all three methods is to use for quantum information processing only a small subset of a larger set of entangled ancilla qubits. Although these ideas are very promising for small register lengths, the techniques become increasingly difficult if one attempts to realize large qubit registers in physical systems. Moreover, one has to keep track of the quantum state of the environment. Whilst these requirements are seemingly feasible for quantum optical information processing systems [37], they appear insufficient for condensed matter systems with their characteristic huge number of environmental degrees of freedom.

An alternative approach consists in minimizing the occurrence of errors by *controlling decoherence* via the application of tailored time-dependent external fields to qubit systems [15,38–41]. For example, the application of a time-dependent periodic external field can induce a Floquet spectrum with degenerate quasienergy states [15,38,39] or it can move the qubit out off resonance with certain bath modes [41] thereby reducing decoherence. The suitability of such schemes to a quantum gate operation, however, remains to be demonstrated.

### ACKNOWLEDGEMENT

We thank Yu. Makhlin and R. Blick for helpful discussions. This work has been supported by the Deutsche Forschungsgemeinschaft via Grant No. HA 1517/19-1.

- 
- [1] D. Deutsch, Proc. R. Soc. Lond. A **425**, 73 (1989); A. Barenco, Proc. R. Soc. Lond. A **449**, 679 (1995); D. DiVincenzo, Phys. Rev. A **51**, 1015 (1995).
  - [2] S. Lloyd, Phys. Rev. Lett. **75**, 346 (1995); D. Deutsch, A. Barenco, and A. Ekert, Proc. R. Soc. Lond. A **449**, 669 (1995).
  - [3] V. Vedral, A. Barenco, and A. Ekert, Phys. Rev. A **54**, 147 (1996).
  - [4] P. W. Shor, in Proceedings of the 35th Annual Symposium on Foundations of Computer Science, ed. by S. Goldwasser (IEEE Computer Society Press, Los Alamitos, CA, 1994); A. Ekert and R. Jozsa, Rev. Mod. Phys. **68**, 733 (1996).
  - [5] D. Deutsch, Proc. R. Soc. Lond. A **400**, 97 (1985).
  - [6] A. Barenco, Ch. H. Bennett, R. Cleve, D. P. DiVincenzo, M. Margolus, P. Shor, T. Sleator, J. A. Smolin, and H. Weinfurter, Phys. Rev. A **52**, 3457 (1995).
  - [7] W. G. Unruh, Phys. Rev. A **51**, 992 (1995).
  - [8] A. Garg, Phys. Rev. Lett. **77**, 964 (1996).
  - [9] G. Massimo Palma, K.-A. Suominen, and A. Ekert, Proc. R. Soc. Lond. A **452**, 567 (1996).
  - [10] R. Landauer, Proc. R. Soc. Lond. A **454**, 305 (1998).
  - [11] D. Loss and D. DiVincenzo, Phys. Rev. A **57**, 120 (1998).
  - [12] Yu. Makhlin, G. Schön, and A. Shnirman, Rev. Mod. Phys. (2001), in press.
  - [13] A. O. Caldeira and A. J. Leggett, Ann. Phys. (N.Y.) **149**, 374 (1983); **153**, 445 (E) (1984); A. J. Leggett, S. Chakravarty, A. T. Dorsey, M. Fisher, A. Garg, and W. Zwerger, Rev. Mod. Phys. **59**, 1 (1987); **67**, 725 (E) (1995).
  - [14] U. Weiss, *Quantum Dissipative Systems* (World Scientific, Singapore, 1993; 2nd edition 1999).
  - [15] M. Grifoni and P. Hänggi, Phys. Rep. **304**, 230 (1998).
  - [16] M. Grifoni, E. Paladino, and U. Weiss, Eur. Phys. J. B **10**, 719 (1999).
  - [17] M. Dubé and P.C.E. Stamp, Int. J. Mod. Phys. B **12**, 1191 (1998).
  - [18] M. Governale, M. Grifoni, and G. Schön, Chem. Phys. **268**, 273 (2001).
  - [19] D. Ahn, J. H. Oh, K. Kimm, and S. W. Hwang, Phys. Rev. A **61**, 052310 (2000).
  - [20] N. G. van Kampen, *Stochastic processes in physics and chemistry* (North-Holland, Amsterdam 1992).
  - [21] A. Suárez, R. Silbey, and I. Oppenheim, J. Chem. Phys. **97**, 5101 (1992).
  - [22] D. E. Makarov and N. Makri, Chem. Phys. Lett. **221**, 482 (1994); N. Makri and D. E. Makarov, J. Chem. Phys. **102**, 4600 (1995); **102**, 4611 (1995); N. Makri, J. Math. Phys. **36**, 2430 (1995).
  - [23] M. Thorwart and P. Jung, Phys. Rev. Lett. **78**, 2503 (1997); M. Thorwart, P. Reimann, P. Jung, and R.F. Fox, Chem. Phys. **235**, 61 (1998).
  - [24] M. Thorwart, P. Reimann, and P. Hänggi, Phys. Rev. E **62**, 5808 (2000).
  - [25] J.F. Poyatos, J.I. Cirac, and P. Zoller, Phys. Rev. Lett. **78**, 390 (1997).

- [26] *The Physics of Quantum Information: Quantum Cryptography, Quantum Teleportation, Quantum Computation*, ed. by D. Bouwmeester, A. Ekert, and A. Zeilinger, (Berlin, Springer 2000).
- [27] J. E. Mooij, T. P. Orlando, L. Levitov, L. Tian, C. H. van der Waal, and S. Lloyd, *Science* **285**, 1036 (1999); T. P. Orlando, J. E. Mooij, L. Tian, C. H. van der Waal, L. Levitov, S. Lloyd, and J. J. Mazo, *Phys. Rev. E* **60**, 15398 (1999); L. Tian, L. Levitov, C. H. van der Waal, J. E. Mooij, T. P. Orlando, S. Lloyd, C. J. P. M. Harmans, and J. Mazo, in Proceedings of the NATO-ASI on "Quantum Mesoscopic Phenomena and Mesoscopic Devices in Microelectronics", cond-mat/99100062; C. H. van der Waal, A. C. ter Haar, F. K. Wilhelm, R. N. Schouten, C. J. P. M. Harmans, T. P. Orlando, S. Lloyd, and J. E. Mooij, *Science* **290**, 773 (2000); J. R. Friedman, V. Patel, W. Chen, S. K. Tolpygo, and J. E. Lukens, *Nature* **406**, 43 (2000); G. Blatter, *ibid.* **406**, 25 (2000); L. B. Ioffe, V. B. Geshkenbein, M. V. Feigel'man, A. L. Fauchère, and G. Blatter, *Nature* **398**, 679 (1999); G. Blatter, V. B. Geshkenbein, and L. B. Ioffe, preprint cond-mat/9912163.
- [28] D. V. Averin, *Solid State Commun.* **105**, 659 (1998); Yu. Makhlin, G. Schön, and A. Shnirman, *Nature* **398**, 305 (1999); V. Bouchiat, D. Vion, P. Joyez, D. Esteve, and M. Devoret, *Physica Scripta* **T76**, 165 (1998); Y. Nakamura, Y. Pashkin, and J. Tsai, *Nature* **398**, 786 (1999); D. Averin, *ibid.* **398**, 748 (1999).
- [29] G. Burkard, D. Loss, and D. P. DiVincenzo, *Phys. Rev. B* **59**, 2070 (1999); A. Imamoglu, D. D. Awschalom, G. Burkard, D. P. DiVincenzo, D. Loss, M. Sherwin, and A. Small, *Phys. Rev. Lett.* **83**, 4204 (1999); X. Hu and S. Das Sarma, *Phys. Rev. A* **61**, 062301 (2000); S. Bandyopadhyay, *Phys. Rev. B* **61**, 13813 (2000); J. Levy, preprint quant-ph/0101026.
- [30] R. Blick and H. Lorenz, Proceedings of the IEEE International Symposium on Circuits and Systems, May 28-31, 2000, Geneva Switzerland, ISCAS 2000, pp. II245-II 248; # 1338.PDF on CD-ROM (ISBB 0-780-5485-0); A. W. Holleitner, C. R. Decker, K. Eberl, and R. H. Blick, preprint cond-mat/0011044; M. Bayer, P. Hawrylak, K. Hinzer, S. Fafard, M. Korkusinski, Z. R. Wasilewski, O. Stern, and A. Forchel, *Science* **291**, 451 (2001); J. H. Reina, L. Quiroga, and N. F. Johnson, in *Proceedings of the ISI-Accademia dei Lincei Conference "Conventional and non Conventional Computing (Quantum and DNA)"*, (Berlin, Springer 2001).
- [31] V. Privman, I. D. Vagner, and G. Kventsel, *Phys. Lett. A* **239**, 141 (1998); B. E. Kane, *Nature* **393**, 133 (1998); D. P. DiVincenzo, *ibid.* **393**, 113 (1998); R. Vrijen, E. Yablonoitch, K. Wang, H. W. Jiang, A. Balandin, V. Roychowdhury, T. Mor, and D. P. DiVincenzo, *Phys. Rev. A* **62**, 012306 (2000); D. Mozysky, V. Privman, and I. D. Vagner, *Phys. Rev. B* **63**, 085313 (2001).
- [32] V. Privman, D. Mozysky, and I. D. Vagner, preprint cond-mat/0102308.
- [33] R. Ionicioiu, G. Amaratunga, and F. Udrea, *Int. J. Mod. Phys. B* **15**, 125 (2001).
- [34] R. P. Feynman and F. L. Vernon Jr., *Ann. Phys. (N.Y.)* **24**, 118 (1963).
- [35] Ch. H. Bennett, G. Brassard, S. Popescu, B. Schuhmacher, J. A. Smolin, and W. K. Wootters, *Phys. Rev. Lett.* **76**, 722 (1996).
- [36] A. Peres, *Phys. Rev. Lett.* **77**, 1413 (1996); M. Horodecki, P. Horodecki, and R. Horodecki, *Phys. Lett. A* **223**, 1 (1996).
- [37] C. J. Myatt, B. E. King, Q. A. Turchette, C. A. Sackett, D. Kielpinski, W. M. Itano, C. Monroe, and D. J. Wineland, *Nature* **403**, 269 (2000); W. Schleich, *ibid.* **403**, 256 (2000).
- [38] T. Dittrich, B. Oelschlägel, and P. Hänggi, *Europhys. Lett.* **22**, 5 (1993).
- [39] P. Hänggi, in *Quantum Dynamics of Submicron Structures*, ed. by H. A. Cerdeira, G. Schön and B. Kramer, NATO ASI Series Vol. E 291, (Boston, Kluwer 1995).
- [40] L. Viola, E. Knill, and S. Lloyd, *Phys. Rev. Lett.* **82**, 2417 (1999); L. Viola, S. Lloyd, and E. Knill, *Phys. Rev. Lett.* **83**, 4888 (1999).
- [41] M. Thorwart, L. Hartmann, I. Goychuk, and P. Hänggi, *J. Mod. Opt.* **47**, 2905 (2000).

Set	$B^z$	$B^x$	$J$	$T$	$B^x/B^z$	$J/B^z$	$T/B^z$
I: Flux qubits	0.5 K	50 mK	25 mK	25 mK	0.1	0.05	0.05
II: Charge qubits	1 K	100 mK	5 mK	50 mK	0.1	0.005	0.05
III: Quantum dot qubits	1 meV	1 meV	0.05 meV	125 mK	1	0.05	0.01

TABLE I. Parameter sets which have been used for the simulations of the quantum XOR gate. They mimic typical experimental situations in three important solid-state qubit systems, i.e., flux qubits and charge qubits in superconducting Josephson devices (Set I and II) and spin and charge qubits in ultrasmall semiconductor quantum dots (Set III).

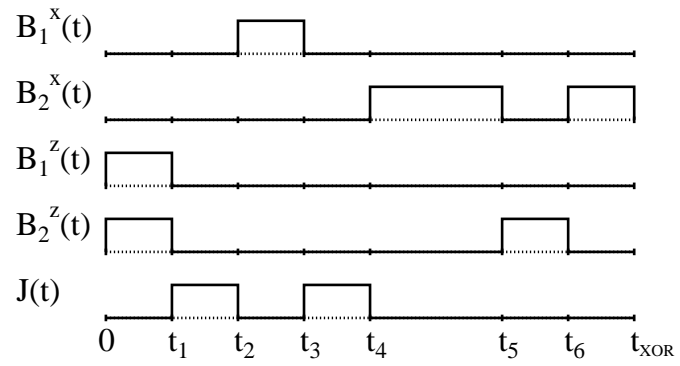


FIG. 1. Schematic view of a pulse sequence necessary to generate the quantum XOR gate. The parameters are set to  $B^x = B^z = J = \text{const.}$ . The frequencies are given in units of  $B^z$  while the time is scaled in units of  $(B^z)^{-1}$ . The switching times  $t_j$  are given in the text and are in this case equal to multiples of  $\pi/2$ .

### XOR gate: $T=0.1$ , $\omega_c=50$

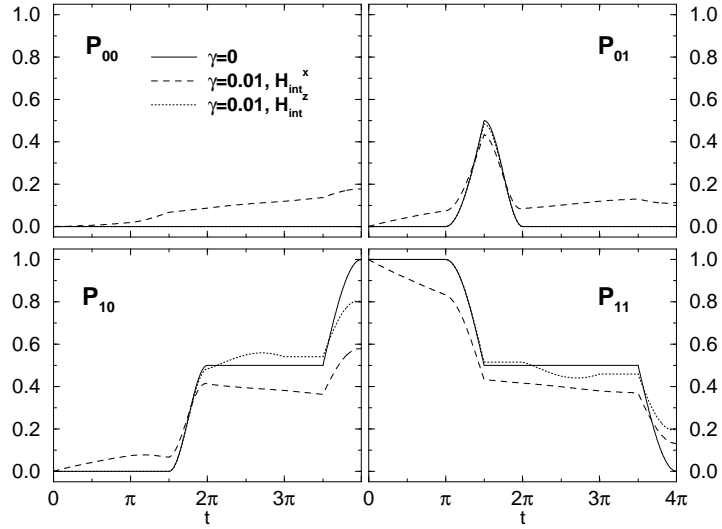


FIG. 2. Time resolved dynamics of the quantum XOR operation for the case of equal energies, i.e.,  $B^x = B^z = J$ . Depicted are the populations  $P_{ij}(t) = \langle ij | \rho(t) | ij \rangle$  as a function of time for the initial condition  $\rho(0) = |11\rangle\langle 11|$  for three different cases of (i) no damping,  $\gamma^{x/z} = 0$ , (solid line), (ii) bit flip errors with  $\gamma^x = 0.01$  (long dashed line), and (iii) phase errors with  $\gamma^z = 0.01$  (dotted line). The time is scaled in units of  $(B^z)^{-1}$ . Moreover, we set the temperature to  $T = 0.1\hbar B^z/k_B$  and the cut-off frequency to  $\omega_c = 50B^z$ .

### Dependence on temperature

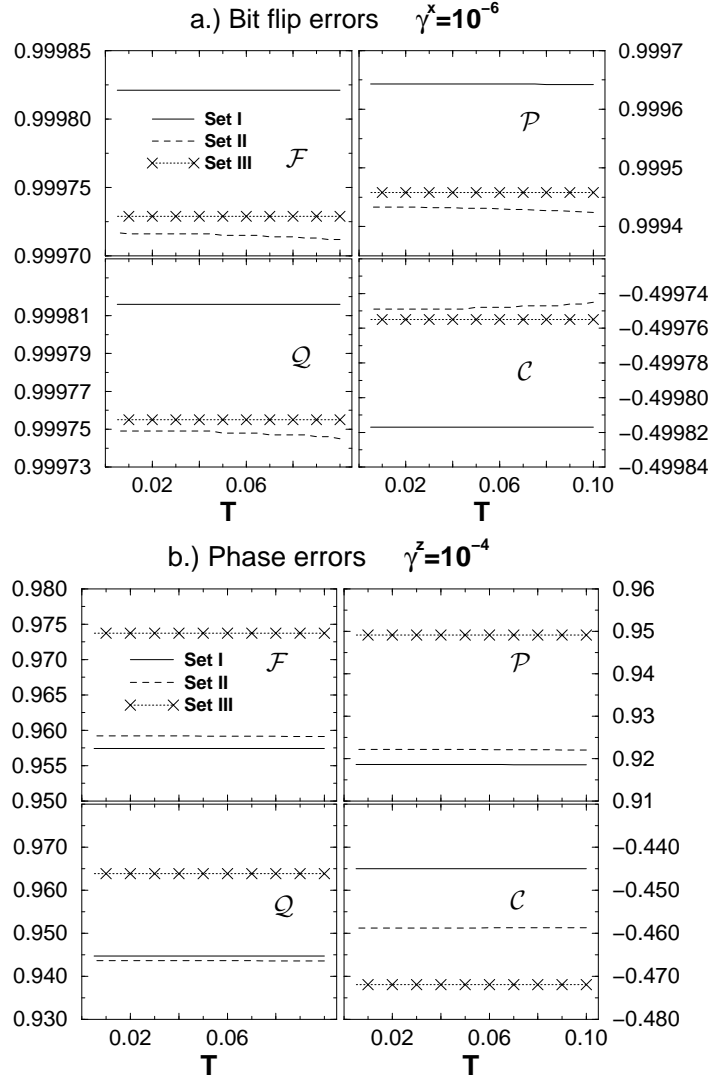
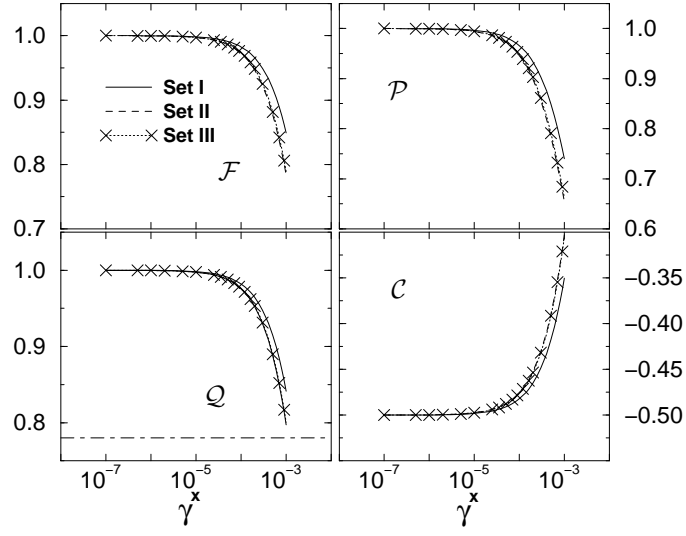


FIG. 3. Dependence of the fidelity  $\mathcal{F}$ , the purity  $\mathcal{P}$ , the quantum degree  $\mathcal{Q}$ , see (18 - 20) and the entanglement capability  $\mathcal{C}$  on temperature  $T$  for bit flip errors (Fig. 3 a.) and phase errors (Fig. 3 b.). The temperature is scaled in units of  $\hbar B^z/k_B$ . The qubit parameters are given in Table I. The damping constant for the bit flip errors is set at  $\gamma^x = 10^{-6}$  and for the phase errors at  $\gamma^z = 10^{-4}$ .

## Dependence on friction strength

### a.) Bit flip errors



### b.) Phase errors

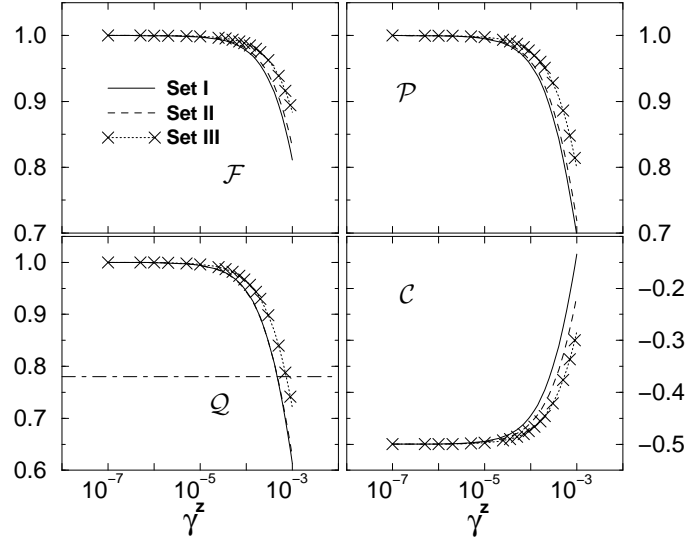


FIG. 4. Dependence of the four gate quantifiers on the dimensionless friction strength. Upper panel a.): Bit flip errors ( $\gamma^x$ ), lower panel b.): Phase errors ( $\gamma^z$ ). The lower bound of  $\mathcal{Q} \approx 0.78$  for the Clauser-Horne-Shimony-Holt inequality is indicated by the horizontal dotted-dashed line (see text). For the remaining parameters, see Table I.

## Dependence on interqubit coupling

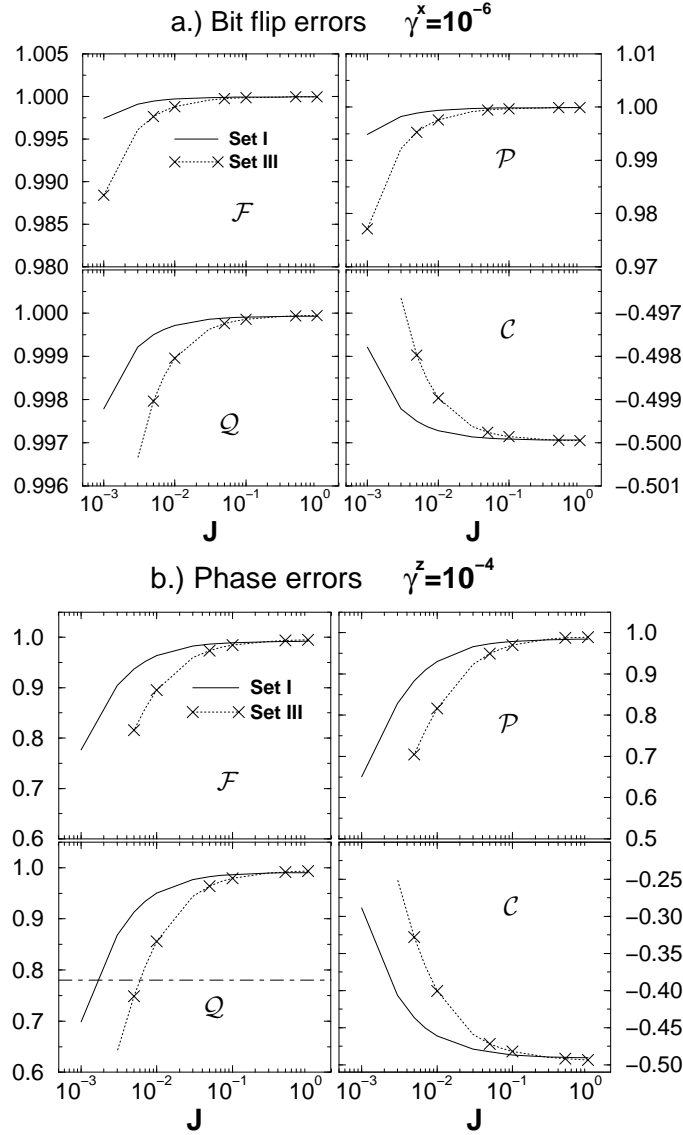


FIG. 5. Dependence of the gate quantifiers on the strength  $J$  of the interqubit coupling. Depicted are the results for parameter set I and III from Table I. The upper panel a.) shows the results for the bit-flip error with  $\gamma^x = 10^{-6}$  while the lower panel b.) depicts the results for the phase error with  $\gamma^z = 10^{-4}$ . The horizontal dotted-dashed line marks the lower bound of  $Q \approx 0.78$  for the Clauser-Horne-Shimony-Holt inequality.